Hindawi
Journal of Sensors
Volume 2021, Article ID 5580847, 10 pages
https://doi.org/10.1155/2021/5580847

Research Article

An Improved Prony Prediction Compensation-Based Wide-Area Damping Control Approach for Power System Low-Frequency Oscillation Suppression

Shujun Chang,[1] **Chao Peng**,[2,3] **Yuyang Hu**,[2] **and Yaxue Mou**[2]

[1]*University of Electronic Science and Technology of China Zhongshan Institute Zhongshan, Zhongshan, Guangdong 528400, China*
[2]*School of Automation Engineering, University of Electronic Science and Technology of China, Chengdu, Sichuan 610054, China*
[3]*Intelligent Terminal Key Laboratory of Sichuan Province, Yibin, Sichuan 644000, China*

Correspondence should be addressed to Shujun Chang; sannychang@zsc.edu.cn and Chao Peng; pcddiy@163.com

Received 7 January 2021; Revised 2 June 2021; Accepted 21 August 2021; Published 10 September 2021

Academic Editor: Gabriele Cazzulani

Currently, wide-area damping control has been considered one of the most effective and promising methods to solve the problem of interval low-frequency oscillation in power systems. In order to reduce adverse affection caused by time delay in acquisition and transmission of wide-area signals, an improved Prony prediction compensation-based wide-area damping control approach for power system low-frequency oscillation suppression is proposed in this paper. Firstly, the influence of communication time delay on power system stability is analyzed by a small disturbance stability analysis method. An algorithm based on the improved Prony prediction algorithm is designed to predict the acquired signals with time delay. A second derivative-based order determination algorithm is used to obtain the best effective order of the prediction model, and the parameter prediction step size of the prediction model is determined by the actual situation of time delay change. Finally, design of a wide-area damping controller based on the improved Prony prediction compensation is presented in detail. The proposed control approach is conducted in a four-machine and two-zone power system, and the experiment results show that the proposed approach can effectively compensate for the signal under the conditions of fixed time delay and variable time delay and has better adaptability advantages than the traditional Prony prediction compensation method.

1. Introduction

Recently, with rapid development of power grids, the scale of power grids is increasing, more and more wide-area complex power grids are built, low-frequency oscillation [1], which threatens safe and stable operation of large-scale power grids, has widely received much attention in industry. Increase in electrical load and distance would exacerbate the problem of low-frequency oscillation. Meanwhile, as an informatization process of the power grid, a huge communication system has gradually become the "vessel" of the power system, carrying the important large-volume information transmission. Long-distance and network uncertainty will introduce time-varying time delays which also bring challenge to low-frequency oscillation suppression and power system stability.

The low-frequency oscillation problem is closely related to the insufficient damping of the system. The main ideas of its solution are reducing negative damping and increasing positive damping of the power system as soon as possible when the presence of low-frequency oscillations of the power grid is detected. According to the difference of the above principle, solution methods for low-frequency oscillation suppression could be classified into grid structure optimization, high-voltage direct current (HVDC) transmission strategy, flexible AC transmission technology [2, 3], damping control [4–6], and so on. Among them, damping control is considered the most widely used and effective method.

Damping control utilizes a power system stabilizer (PSS) installed at the excitation end, which controls the excitation system to form an electrical torque component in the same phase with the rotor speed deviation to improve the dynamic

performance of the power system. With the application of the Wide-Area Measurement System (WAMS), remote signals such as voltage, current, frequency, and other phasor information can be used for wide-area power system damping control [7]. However, the acquisition of remote signals depends on the main components of WAMS—the communication system—and the information acquisition equipment, the Phasor Measurement Unit (PMU), in the electrical quantity acquisition, data calculation and processing, signal exchange, and execution process. There may be a time delay of up to hundreds of milliseconds [8]. Therefore, in order for the system to operate stably, damping control using remote signals is an effective way to suppress the low-frequency oscillations of the power system, especially the interval oscillations [9–12]. Thus, for a wide-area complex power grid, the time delay problem of damping control is unavoidable. The time delay problem will seriously affect the performance of the power system stabilizer, and in severe cases, the stabilizer will not be able to provide sufficient damping for the interval low-frequency oscillation.

Currently, the research on power system damping control mainly focuses on the analysis of time delay characteristics and the design of damping controllers considering the wide-area signal time delay. According to the design idea, the existing damping control approaches could be classified into a robust control-based approach and time delay compensation-based control approach. Robust control-based approaches utilize robust control and optimization theory to reduce system sensitivity to time delay and improve system stability, such as a Lyapunov-Krasovskii theory-based robust control [13], $H\infty$ control-based robust control approach [14], operating condition linearization and model uncertainty consideration-based controller design approach [15, 16], particle swarm optimization-based controller design approach [17, 18], oscillation mode prediction and system identification-based adaptive control approach [19], and Q-learning-based control approach [20]. A time delay compensation-based control approach utilizes time delay equivalence, time delay compensation, and signal prediction in a control scheme to compensate for the time delay, such as variable weighting sequence-based predictive control approach [21], shaped loop transmission function-based compensation approach [22], polynomial fitting predictive compensation approach [23], adaptive compensator-based control [24], increment autoregression prediction-based compensation [25], and unified Smith predictor compensation-based control [26].

As seen above as two types of control approach, the robust control-based damping control approach relies on accurate system models and fixed time delay models are often used in the derivation of criteria. It is difficult to directly apply to engineering, and it is conservative in terms of time delay changes and system model changes. The time delay compensation-based control approach has the following three merits: (1) it can fit the signal conforming to the sinusoidal attenuation characteristics to ensure sufficient accuracy, (2) it can calculate accurate signal compensation before the disturbance causes damage, and (3) prediction does not depend on the precise model of the system. By comparing two of them, the time delay compensation-based control can deal with the adverse effects of time delay on wide-area damping control, which can better adapt to engineering applications and time delay changes.

The Prony algorithm [27] can describe the attenuated triangular signal as a set of linear combinations of exponential functions, and the common input of wide-area PSS includes the speed, power angle, frequency, and other signals of the interval mode dominating the unit. These signals are composed of attenuated trigonometric functions, and the Prony algorithm could be used to predict and compensate for the measured input signal of PSS accurately. Therefore, this paper will introduce the wide-area damping control system structure considering the time delay, the improvement of the Prony prediction algorithm, and the wide-area PSS to construct a wide-area damping control scheme. Based on these works, an improved Prony prediction compensation-based wide-area damping control approach is proposed, and it improves the accuracy of the Prony model, improves the calculation speed of the effective rank of the sample matrix and the accuracy of the prediction step size, and uses the Prony identification algorithm to tune the wide-area PSS parameters, making the control method proposed in this paper more suitable for engineering applications. The effectiveness of the proposed method is verified by a simulation experiment in a four-machine two-zone system.

2. Principle of the Proposed Control Approach

2.1. Stability Analysis Based on Small Disturbance Stability. The state space expression of the N-machine system is described as follows:

$$\begin{cases} \dot{x}(t) = Ax(t) + \mathrm{Bu}(t), \\ y(t) = Cx(t). \end{cases} \tag{1}$$

According to the characteristic equation $\lambda I - A = 0$, all characteristic roots $\lambda_1, \lambda_2, \cdots \lambda_N$ are obtained to describe the operation of the system at the corresponding linearized operating point. Physically, the i-th pair of conjugate characteristic roots of the system describes the i-th mode of oscillation operation of the multimachine system. Corresponding to the eigenvalue of the i-th pair, $\lambda_i = \partial_i \pm j\Omega_i$ is defined as follows:

$$\begin{cases} f_i = \dfrac{\Omega_i}{2\pi}, \\ \sigma_i = \dfrac{-\partial_i}{\sqrt{\partial_i{}^2 + \Omega_i{}^2}}. \end{cases} \tag{2}$$

Then, the low-frequency oscillation mode can be judged according to the correlation ratio of the electromechanical loop. If the characteristic value λ_i meets the following two conditions, it can be called the low-frequency oscillation

operation mode:

$$\begin{cases} \rho_i = \left| \dfrac{\sum_{x_i \in (\Delta\delta, \Delta\omega)} P_{ki}}{\sum_{x_i \notin (\Delta\delta, \Delta\omega)} P_{ki}} \right| > 1, \\ \Omega_i \in 0.2 - 2.5\,\text{Hz}, \end{cases} \tag{3}$$

where P_{ki} is the physical quantity that describes the participation degree of the K-th state variable related to the eigenvector corresponding to mode λ_i, and the electromechanical loop correlation ratio calculates the participation degree of $\Delta\delta$ and $\Delta\omega$ state variables in the i-th mode of operation.

2.2. Principle of the Prony Prediction Model. The Prony prediction compensation algorithm is based on the following hypothetical data model:

$$x(t) = \sum_{k=1}^{p} A_k e^{\alpha_k t} \cos\left(2\pi f_k t + \theta_k\right). \tag{4}$$

Assuming that the sampling interval of the data is T_s, let $t = nT_s$; the discrete function expression of the Prony prediction model is obtained according to Euler's formula:

$$\hat{x}[n] = \sum_{k=1}^{p} A_k e^{j\theta_k} \exp\left(\left(\alpha_k + j2\pi f_k\right) T_s n\right) = \sum_{k=1}^{p} h_k z_k^n \quad (n = 1, \cdots, N-1). \tag{5}$$

The characteristic polynomial of the n-th sampling point's estimated value is obtained as follows:

$$\varphi(z) = \prod_{k=1}^{p} (z - z_k) = \sum_{k=0}^{p} a[k] z^{p-k}, \quad a[0] = 1, \tag{6}$$

where z_k is the k-th root of the characteristic polynomial.

By solving the roots and parameters of the Prony polynomial, the frequency, attenuation factor, amplitude, and initial phase of each signal can be calculated as follows:

$$\begin{cases} \alpha_k = \dfrac{\ln |z_k|}{T_s}, \\ f_k = -\dfrac{\tan^{-1}\left[\text{Im}\,(z_k)/\text{Re}\,(z_k)\right]}{2\pi T_s}, \\ A_k = |h_k|, \\ \theta_k = \tan^{-1}\left[\dfrac{\text{Im}\,(h_k)}{\text{Re}\,(h_k)}\right]. \end{cases} \tag{7}$$

Thus, the Prony prediction model is obtained. When the actual data is relatively small, the Prony method can complete the local prediction at the current position. As the sampling time and the number of data increase, the Prony method can identify all the oscillation modes and predict the data for a long time. Assuming that the prediction step size is k, the prediction model is

$$\hat{x}[N + k] = \sum_{k=1}^{p} h_k z_k^{(N+k-1)}. \tag{8}$$

2.3. Structure of the Proposed Control Approach. The main equipment of the wide-area damping control system based on a predictive compensation algorithm includes PMU, network control unit, control center, and communication network, and its structure is shown in Figure 1.

The processing of measurement data, time delay analysis and calculation, and predictive compensation of the controller input signal are all performed in the control center. So, the proposed damping control approach will be implemented in the control center. The main idea of the proposed damping control approach is to calculate the power angle difference that needs to be compensated between the regional units according to the output signal and design the WPSS parameters according to the phase compensation method, which can achieve a good suppression effect of interval low-frequency oscillation without considering the time delay. Then, the Prony predictive compensation algorithm is used to calculate a set of predictive data queues based on the measured relative angular velocity data, and finally the appropriate data is selected from the predictive data queue as the input of WPSS according to the local time stamp of the controller.

2.4. Wide-Area Closed-Loop Control System Model considering Time Delay. The power system stabilizer used in this paper represents the general form of the transfer function of the wide-area damping controller, which can be written in the following form:

$$H_{\text{wpss}}(s) = K_w \frac{T_w s}{1 + T_w s} \left(\frac{T_1 s + 1}{T_2 s + 1}\right)^m, \tag{9}$$

where m represents the number of leading and lagging links, T_w is the time constant of the power system, K_w is the gain of the PSS, and T_1 and T_2 are the leading and lagging time constants calculated.

The damping controller can be represented by the following state space model:

$$\begin{cases} \dot{x}_1(t) = A_1 x_1(t) + B_1 u_1(t), \\ y_1(t) = C_1 x_1(t) + D_1 u_1(t), \end{cases} \tag{10}$$

where $u_1(t)$ is the remote measured signal used by the controller, D_1 is the direct transfer function coefficient, $y_1(t)$ represents the control output of the controller, $x_1(t)$ is the state vector of the control system, and A_1, B_1, C_1, and D_1 are the corresponding system state matrix.

The time synchronization function provided by WAMS will mark the measured data packet with the time stamp t_s and synchronize the time of all devices in the system. According to this feature, compare the time stamp of the measured data packet and the current time when the data

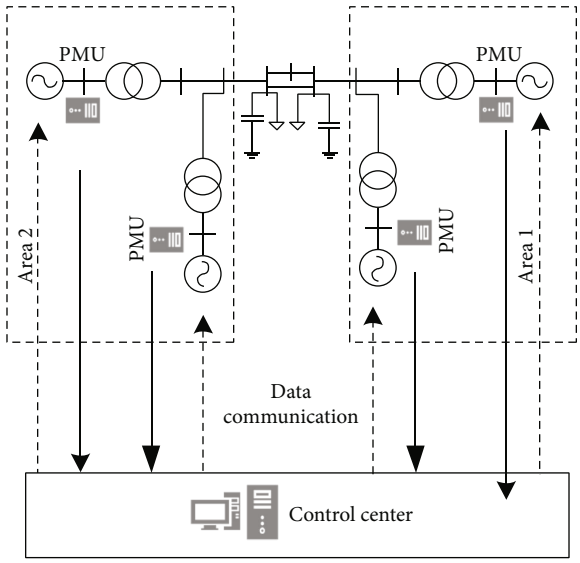

Figure 1: Wide-area closed-loop control framework and information flow based on a two-area system.

packet arrives at the WPSS input terminal to get the time delay t_e. Then, wide-area signal communication delay could be written as

$$\tau = t_s - t_e. \tag{11}$$

The wide-area closed-loop control system including the wide-area power system, wide-area damping control system, and communication delay can be expressed as the following model, and the structure diagram is shown in Figure 2.

$$\dot{x}(t) = A_c x(t) + A_d x(t-\tau), \tag{12}$$

where $x = [x_1, x_2]^T$,

$$A_c = \begin{bmatrix} A & BC \\ 0 & A_1 \end{bmatrix}, \quad A_d = \begin{bmatrix} BD_1C & 0 \\ B_1C & 0 \end{bmatrix}. \tag{13}$$

3. Design of the Improved Prony Prediction Algorithm

3.1. Second Derivative-Based Order Determination Algorithm. From the analysis of the theoretical part of the Prony prediction algorithm, it can be seen that the order of the sample matrix is the key to obtaining an accurate Prony prediction model. If the order is too high, many noncritical modes will be introduced, which will affect the accurate extraction of key modes. If the value is too low, some important mode information will be lost. Generally speaking, the order of the system is unknown before being identified. A normalized singular value method (NSVM) threshold based on the normalized ratio method to determine the fitting order is introduced in [28]. However, the normalized ratio method will perform full-order calculations, and choosing an appropriate threshold in NSVM is the key to improving Prony's accuracy. If the threshold is selected too large, important information will be lost or even lead to system identification failure. The order of the fitting system is too low. If the threshold is selected too small, it will seriously increase the computational burden and produce a large number of redundant modes.

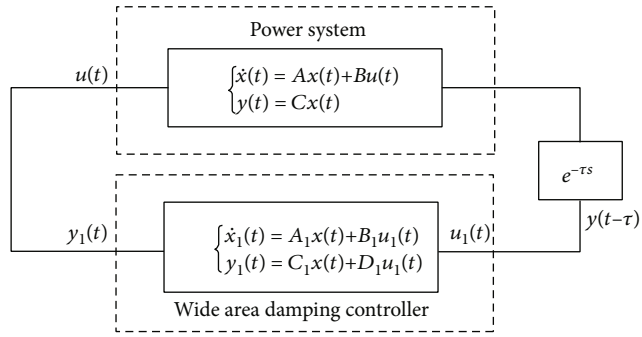

Figure 2: Wide-area power system damping control system with time delay.

Therefore, this paper introduces a second derivative method into the Prony algorithm to determine the optimal order of system fitting to obtain the accurate Prony prediction model. The steps of determining the optimal order by using the second derivative method are as follows:

Step 1. The singular value of the sample matrix R is solved, and the calculated result $\zeta_i (i = 1, 2, \cdots, p_w)$ is written as $\zeta_1 \geq \zeta_2 \geq \zeta_p \geq \cdots \geq \zeta_{pw} \approx 0$ after permutation.

Step 2. The singular value $\zeta_i (i = 1, 2, \cdots, p_w)$ of the sample matrix R has the characteristics of large numerical differences. The singular value before the optimal order P is large, while the singular value after the order P will decrease sharply. The values $(p_w - p)$ of the latter half of the sequence are very small with a small rate of change, so it can be considered that this part corresponds to the interference signal.

Step 3. According to the formula of $\nabla^2\zeta(j) = \zeta(j) - 2\zeta(j-1) + \zeta(j-2)$, calculate the second-order difference corresponding to each point in the singular value sequence from $j = 1$, where $\zeta(j)$ is the j-th singular value. When j increases to the initial order p_w of the model and $|\nabla^2\zeta(j)|$ decreases to zero, the corresponding j is singular value mutation points, namely, the critical point between the optimal order and the jamming signal, then continue to calculate the Prony model parameters after calculating the system effective order.

3.2. Compensation Step Prediction

3.2.1. Time Delay Measurement. Assuming that the data measured by the PMU at time is t_s, the data is sent to the control center every 10 ms, that is, the sampling time T_s = 10 ms, and the sent data will contain the time stamp of the

measurement time t_e. The data transmission process with time-varying delay is shown in Figure 3.

The control center will arrange the actual data measured by the PMU according to the size of the time scale and store it in a queue. Assuming that the data with the time stamp sent by the PMU is received at the current moment, the data delay can be calculated using the local time and time stamp of the control center. This article divides the data transmission delay process into the following three categories:

(1) For example, as shown in Figure 3, data 1 arrives at the receiving end within a sampling period after being sent from the starting end. At this time, it can be considered that the data is transmitted normally, and the effect of delay can be ignored, which is equivalent to 0

(2) If the data is sent at any time and is received at a time other than the sending sampling period, there will be a delay

(3) When different data arrive at the same sampling time, such as data 2 and data 3, the control center selects the data that arrives first and other data will be rejected

In general, this article considers three transmission situations: normal transmission, transmission delay, and data rejection. According to these three situations, the delay time can be standardized to handle more complex data transmission situations.

3.2.2. Determination of the Prediction Step. In this paper, the data transmission time delay process is divided into three cases: the delay caused by normal transmission, the delay caused by transmission delay, and the delay caused by data rejection. Then, according to the characteristics of the time delay sequence, a maximum predictive time delay $T_{\max}$ is set, and the prediction step within the sampling interval of each round is $T = \lceil T_{\max}/\Delta t \rceil$, where $\lceil \rceil$ represents the upward integration. In addition, the actual time delay at the current moment is called the predictive time.

Then, according to the Prony prediction model (equation (8)), data can be predicted and extrapolated:

$$\begin{aligned}&(\widehat{w}[k+1], \widehat{w}[k+2], \cdots, \widehat{w}[k+L])\\ &\quad = \text{prony}(w[k-K+1], \cdots, w[k-1], w[k]).\end{aligned} \tag{14}$$

prony$(\cdot)$ represents the function of the Prony prediction algorithm, K is the length of the historical angular velocity data sequence, and $w[k-K+1], \cdots, w[k-1], w[k]$ is the historical angular velocity data sequence. It includes the angular velocity signal $w[k]$ received by WPSS at the current moment, and $\widehat{w}[k+1], \widehat{w}[k+2], \cdots, \widehat{w}[k+L]$ represents L data obtained from the prediction compensation of the Prony prediction model.

Then, according to the time delay τ_{pk} corresponding to the current moment, calculate the prediction compensation step of the current moment which is $L_{pk} = \tau_{pk}/\Delta t$ and select

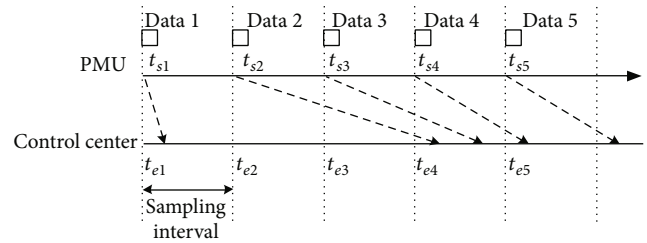

FIGURE 3: Data transmission process with time-varying delay.

$\widehat{w}[k+n] = \min\{|n - L_{pk}|\}$ from $\widehat{w}[k+1], \widehat{w}[k+2], \cdots, \widehat{w}[k+L]$ as the input of controller WPSS.

4. Design of the Improved Prony Prediction Compensation-Based Wide-Area Damping Controller

The design of the wide-area controller based on the improved Prony prediction compensation algorithm is shown as follows:

Step 1. Firstly, a small disturbance is applied to the power system object to stimulate the low-frequency oscillation mode, and the signal that can be used as the input of WPSS is collected, which can be the power angle, angular velocity, and active power signal of each unit. In this paper, the angular velocity signal difference between units is selected as the feedback signal of the wide-area closed-loop system.

Step 2. The WPSS parameters which can effectively suppress the interval oscillation mode of the power system are determined by using the phase compensation method without considering the time delay.

Step 3. The order of the sample matrix based on the Prony algorithm is calculated by using the recorded sampling data at equal time intervals, namely, the order reduction of the dominant mode of the system which is determined.

Step 4. Using the characteristics of WAMS to transmit data packets with time scale information, the prediction step estimation module of the control center subtracts the data time scale with local time, does statistics on the measurement results of time delay, and updates the predicted step size.

Step 5. Before the arrival of the next sampling data, the Prony prediction model is calculated according to the Prony algorithm, the prediction compensation data is extrapolated according to the preset value, and the appropriate prediction data is selected according to the current actual time delay and transmitted to the input end of the wide-area damping controller.

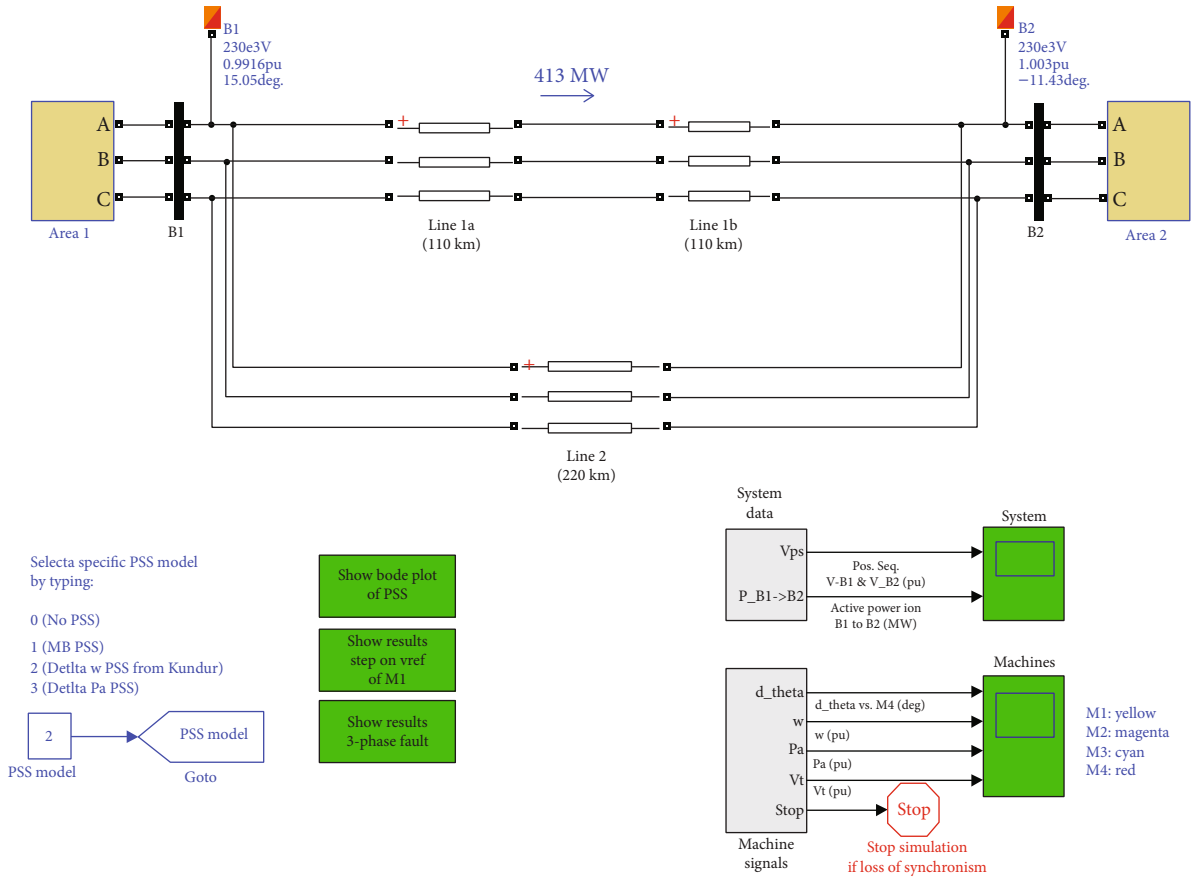

Figure 4: Four-machine and two-zone system Simulink model.

5. Experiment Results and Discussion

This paper will prove that the Prony prediction compensation algorithm can solve the phase lag problem caused by time delay on the basis of the four-machine and two-zone system [13, 14]. As shown in Figure 4, the experiment adopted a four-machine and two-zone system equipped with local PSS, supposing that the generator adopted a third-order practical model and the excitation system adopted a third-order model [16]. The simulation step size of Simulink is set as 0.01 s.

The electromechanical mode of the four-machine and two-zone system is shown in Table 1.

The analysis shows that the calculation example has two local modes (mode 1 and mode 2) and one interval mode (mode 3). The damping ratio of mode 3 is less than 3%, and the frequency is in the range of 0.2~2.5 Hz. It is in the low-frequency oscillation mode. It is the interregional low-frequency oscillation mode and requires additional damping control equipment to provide additional damping. Analyzing the geometric controllable and observable index shows that the dominant units in mode 3 are generator 1 and generator 4. Therefore, generator 1 is selected to add angular velocity-type PSS as the wide-area damping controller to suppress this oscillation mode, and the feedback signal is generator 3 angular velocity.

According to the identification and analysis results, the parameters of the wide-area damping controller could be designed as follows:

$$H(s) = 5.8\frac{10s}{1+10s}\left(\frac{1.1126s+1}{0.6387s+1}\right)^2. \quad (15)$$

5.1. Wide-Area Damping Control Experiment with Fixed Time Delay. A fixed time delay of 0.2 s was added to the system. During the simulation process, the generator speed signal was sampled once every period of time to calculate the angular velocity of generator 3, simulating the process of PMU acquisition and transmission signal. The time window was set as 1 s and the sampling interval was set as 20 ms to take the sampling points. The simulation results are shown in Figure 5.

By observing the angular velocity difference between generator 1 and generator 3, it is found that the oscillation amplitude of the traditional Prony prediction compensation method is slightly larger than that of the improved Prony prediction compensation method. The compensation algorithm based on the improved Prony predicted under the condition of the fixed time delay successfully inhibits the wave oscillation when run about 5 s, the control effect is improved obviously compared with the compensation

Table 1: Electromechanical mode of a four-machine and two-zone system.

Mode	Real part of the characteristic root	Imaginary part of the characteristic root	Damping ratio	Frequency (Hz)	No. of participating generators
1	-0.6393	8.9827	0.071	1.42	No. 3, no. 4
2	-0.6406	9.2689	0.069	1.47	No. 1, no. 2
3	-0.0160	4.4755	0.0036	0.71	No. 1, no. 2, no. 3, no. 4

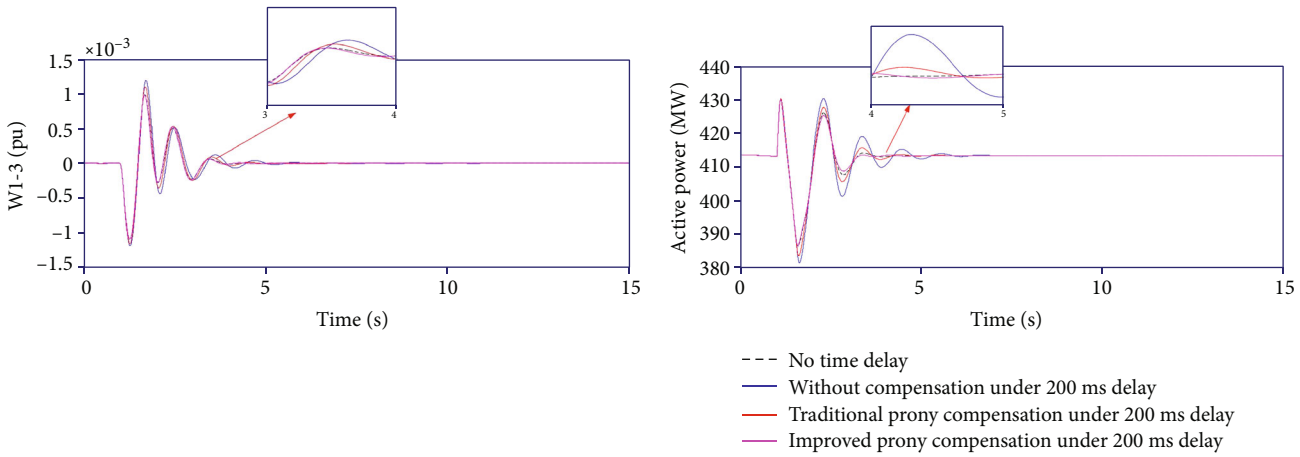

(a) Results of angular velocity difference of G1 and G3

(b) Results of active power of the regional tie line

Figure 5: Comparison of simulation results between the traditional Prony prediction compensation and improved Prony prediction compensation.

without time delay, and the difference is small compared with the wide-area PSS control effect without time delay. It proves that the proposed Prony prediction compensation algorithm can effectively compensate for the fixed time delay and suppress the interval low-frequency oscillation.

5.2. Wide-Area Damping Control Experiment with Variable Time Delay. The two groups of time delay sequences of three different stages are designed, denoted as time delay sequence 1 and time delay sequence 2. The mathematical distribution of time delay signals is shown in Table 2.

For time delay sequence 1, the fixed time delay compensator and the traditional Prony prediction compensation module were set as the control group to compare with the improved Prony prediction compensation algorithm. The time window length and sampling interval of the traditional and improved Prony prediction compensation module are 1 s and 20 ms, respectively. The designed time delay compensator is

$$H_c = 0.7\frac{1+0.68s}{1+0.07s}. \tag{16}$$

The maximum predicted time delay is set as 300 ms, and the fixed compensated time delay is $t = 0.2$s. The simulation results are shown in Figure 6.

For time delay sequence 2, the fixed compensated time delay is $t = 0.2$s. The simulation results obtained are shown in Figure 7.

It can be seen from the comparison of simulation results in the two cases that the system without compensation is always oscillating and cannot be stable. The traditional time delay compensator has a partial compensation effect in the case of variable time delay, but the effect is very limited, so it cannot deal with the situation when the communication condition changes greatly. The improved Prony prediction compensation effect is superior to the traditional Prony prediction compensation effect, but the control time of the two prediction compensation algorithms of time delay sequence 2 is longer than that of time delay sequence 1.

Table 2: Mathematical distribution of time delay sequence 1 and time delay sequence 2.

Time delay sequence	Time interval (s)	Average of delay time (ms)	Standard deviation of delay time (ms)
No. 1	0~5	200	20
	5~10	300	30
	10~15	200	20
No. 2	0~5	200	20
	5~10	200	40
	10~15	200	20

Finally, the comparison result of the actual data and the predicted compensation data of the simulation experiment is shown in Table 3.

As seen in the results in Tables 2 and 3, it can be concluded that the accuracy of the improved Prony prediction compensation algorithm is significantly improved. The maximum errors of the improved Prony prediction

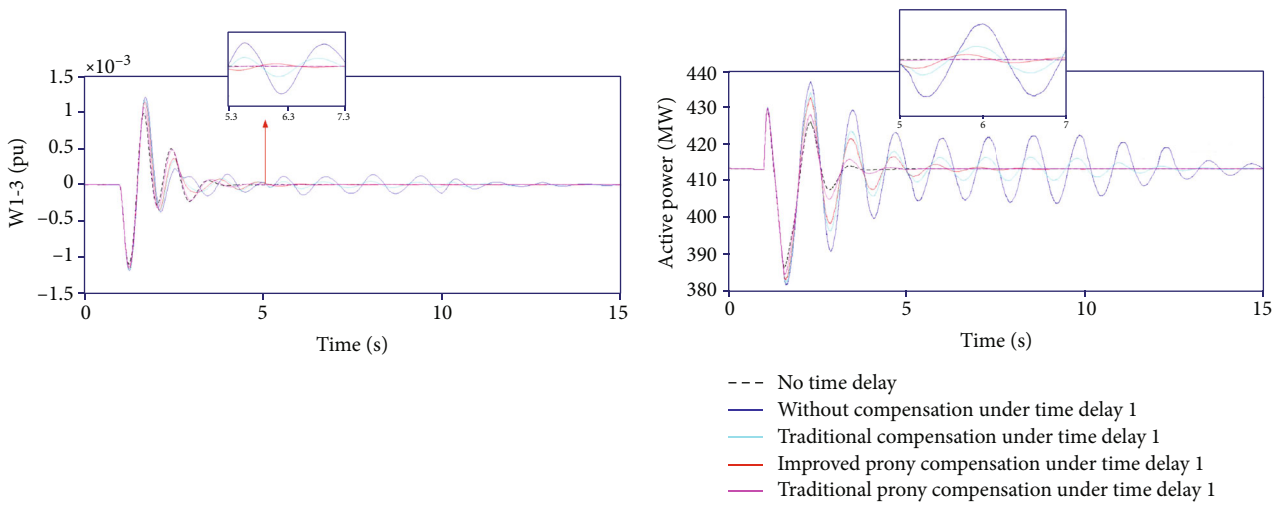

(a) Results of angular velocity difference of G1 and G3

(b) Results of active power of the regional tie line

Figure 6: Comparison simulation of the Prony prediction compensation effect of time delay sequence 1.

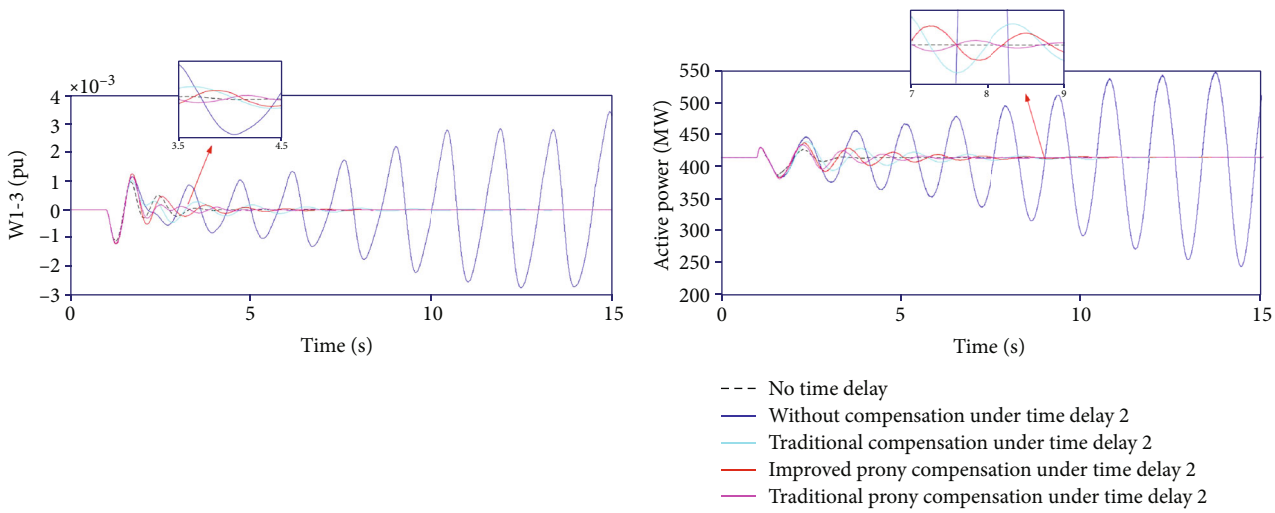

(a) Results of angular velocity difference of G1 and G3

(b) Results of active power of the regional tie line

Figure 7: Comparison simulation of the Prony prediction compensation effect of time delay sequence 2.

Table 3: Prediction error of the Prony prediction compensation under three time delay distributions.

Compensation algorithm	Time delay distribution type	Maximum of error (rad/s)	Root mean square of error (rad/s)	Average of error (rad/s)
Improved Prony compensation	Fixed delay	0.0001	0.0001	0.00004
	Delay sequence 1	0.0015	0.0056	0.00061
	Delay sequence 2	0.0028	0.0079	0.00087
Traditional Prony compensation	Fixed delay	0.0009	0.0041	0.00032
	Delay sequence 1	0.0041	0.0094	0.00098
	Delay sequence 2	0.0063	0.0107	0.00143

compensation algorithm and the traditional Prony prediction compensation algorithm are 0.0028 rad·s^{-1} and 0.0063 rad·s^{-1}, and the maximum RMS errors of the two algorithms are 0.00087 rad·s^{-1} and 0.00143 rad·s^{-1}; they are both in the sequence of time delay 2, which confirms that the delay jitter has played some role in the accuracy of angular velocity data, leading to a drop in the accuracy of the prediction data.

6. Conclusion

With the wide-area damping control of the power system based on WAMS as the background, this paper obtains the following research results and conclusions:

(1) This paper designs the four-machine and two-zone power system model with time delay, and on this basis, experiments show that the wide-area damping control can effectively suppress the interval oscillation mode, improve the small disturbance stability of the system, and prove the necessity of considering the time delay compensation scheme in the controller design

(2) A low-frequency oscillation control method based on the Prony prediction compensation algorithm was improved for the time delay, in which the second derivative method was introduced to improve the Prony algorithm to improve the accuracy of the prediction model and determine the parameter prediction step size of the prediction model. The simulation results show that the proposed method can effectively suppress low-frequency oscillation modes in the case of introducing fixed or variable time delay

Data Availability

The data used to support the findings of this study are included within the article.

Conflicts of Interest

The authors declare that they have no conflicts of interest.

Acknowledgments

This work was supported by Grant SCITLAB-0008 of the Intelligent Terminal Key Laboratory of Sichuan Province.

References

[1] F. Zhu, H. G. Zhao, Z. H. Liu, and H. Z. Kou, "The influence of large power grid interconnected on power system dynamic stability," *Proceedings of the CSEE*, vol. 27, no. 1, pp. 1–7, 2007.

[2] H. F. Wang, "A unified model for the analysis of FACTS devices in damping power system oscillations. III. Unified power flow controller," *IEEE Transactions on Power Delivery*, vol. 15, no. 3, pp. 978–983, 2000.

[3] H. F. Wang, F. J. Swift, and M. Li, "A unified model for the analysis of FACTS devices in damping power system oscillations. II. Multi-machine power systems," *IEEE Transactions on Power Delivery*, vol. 13, no. 4, pp. 1355–1362, 1998.

[4] F. Wu, J. Wang, J. Pan et al., "Determination of suitable locations for power system stabilizers," *Electric Power*, vol. 49, no. 9, pp. 13–17, 2016.

[5] H. Wu and J. Li, "Parameter setting of PSS based on improved genetic algorithm and the application," *Zhejiang Electric Power*, vol. 35, no. 6, pp. 11–16, 2016.

[6] F. Wu, X. Lu, W. Chen et al., "Research of parameter optimization of power system stabilizer," *Power System Protection and Control*, vol. 5, pp. 40–44, 2010.

[7] Shaobu Wang, Xiangyu Meng, and Tongwen Chen, "Wide-area control of power systems through delayed network communication," *IEEE Transactions on Control Systems Technology*, vol. 20, no. 2, pp. 495–503, 2012.

[8] C. Lu, X. Zhang, X. Wang, and Y. Han, "Mathematical expectation modeling of wide-area controlled power systems with stochastic time delay," *IEEE Transactions on Smart Grid*, vol. 6, no. 3, pp. 1511–1519, 2015.

[9] X. Q. Yang and A. Feliachi, "Stabilization of inter-area oscillation modes through excitation systems," *IEEE Transactions on Power Systems*, vol. 9, no. 1, pp. 494–502, 1994.

[10] M. E. Aboul-Ela, A. A. Sallam, J. D. McCalley, and A. A. Fouad, "Damping controller design for power system oscillations using global signals," *IEEE Transactions on Power Systems*, vol. 11, no. 2, pp. 767–773, 1996.

[11] H. Ni, G. T. Heydt, and L. Mili, "Power system stability agents using robust wide-area control," *IEEE Power Engineering Review*, vol. 22, no. 9, pp. 58–58, 2002.

[12] T. Li, M. Wu, and Y. He, "A novel optimization design for unified power flow controller damping control based on communication latency," *Journal of Circuits and Systems*, vol. 2, pp. 200–205, 2013.

[13] Y. Ma, J. Zhang, and Y. Jiang, "Additional robust damping control of wide-area power system with multiple time delays considered," *Transactions of China Electrotechnical Society*, vol. 32, no. 6, pp. 58–66, 2017.

[14] M. Li and Y. Chen, "A wide-area dynamic damping controller based on robust $H\infty$ control for wide-area power systems with random delay and packet dropout," *IEEE Transactions on Power Systems*, vol. 33, no. 4, pp. 4026–4037, 2018.

[15] M. E. C. Bento, "A hybrid procedure to design a wide-area damping controller robust to permanent failure of the communication channels and power system operation uncertainties," *International Journal of Electrical Power & Energy Systems*, vol. 110, pp. 118–135, 2019.

[16] M. E. C. Bento, "Fixed low-order wide-area damping controller considering time delays and power system operation uncertainties," *IEEE Transactions on Power Systems*, vol. 35, no. 5, pp. 3918–3926, 2020.

[17] M. E. C. Bento, "A hybrid particle swarm optimization algorithm for the wide-area damping control design," *IEEE Transactions on Industrial Informatics*, vol. PP, no. 99, p. 1, 2021.

[18] F. Bai, L. Zhu, Y. Liu et al., "Design and implementation of a measurement-based adaptive wide-area damping controller considering time delays," *Electric Power Systems Research*, vol. 130, pp. 1–9, 2016.

[19] M. Mokhtari and F. Aminifar, "Toward wide-area oscillation control through doubly-fed induction generator wind farms," *IEEE Transactions on Power Systems*, vol. 29, no. 6, pp. 2985–2992, 2014.

[20] J. Duan, H. Xu, and W. Liu, "Q-learning-based damping control of wide-area power systems under cyber uncertainties," *IEEE Transactions on Smart Grid*, vol. 9, no. 6, pp. 6408–6418, 2018.

[21] P. Mahish, A. K. Pradhan, and A. K. Sinha, "Wide area predictive control of power system considering communication delay and data drops," *IEEE Transactions on Industrial Informatics*, vol. 15, no. 6, pp. 3243–3253, 2019.

[22] D. Roberson and J. F. OBrien, "Loop shaping of a wide-area damping controller using HVDC," *IEEE Transactions on Power Systems*, vol. 32, no. 3, pp. 2354–2361, 2017.

[23] Z. Hu, X. Xie, and T. L. Characteristic, "Analysis and polynomial fitting based compensation of the time delays in wide-area damping control system," *Automation of Electric Power Systems*, vol. 29, no. 20, pp. 29–34, 2005.

[24] I. Abdulrahman, R. Belkacemi, and G. Radman, "Power oscillations damping using wide-area-based solar plant considering adaptive time-delay compensation," *Energy Systems*, vol. 12, no. 2, pp. 459–489, 2021.

[25] F. Zhang, L. Cheng, X. Li, and Y. Z. Sun, "A prediction-based hierarchical delay compensation (PHDC) technique enhanced by increment autoregression prediction for wide-area control systems," *IEEE Transactions on Smart Grid*, vol. 11, no. 2, pp. 1253–1263, 2020.

[26] Y. Nie, P. Zhang, G. Cai, Y. Zhao, and M. Xu, "Unified Smith predictor compensation and optimal damping control for time-delay power system," *International Journal of Electrical Power and Energy Systems*, vol. 117, pp. 105670-1–105670-11, 2020.

[27] I. A. I. Al-Naib and K. H. Sayidmarie, "Prediction of channel parameters from amplitude-only data using Prony algorithm," *Electronics Letters*, vol. 45, no. 15, pp. 785-786, 2009.

[28] J. Xiong, W. Xing, and Q. Wan, "Identification of control modes in low frequency oscillation analysis by Prony method," *Journal of Southeast University*, vol. 38, no. 1, pp. 64–68, 2008.